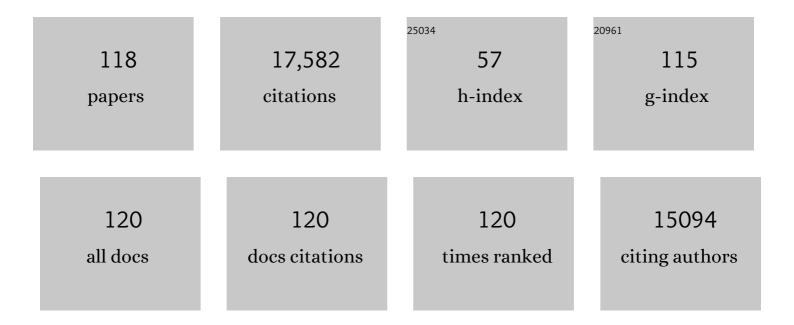
List of Publications by Year in descending order

Source: https://exaly.com/author-pdf/9148019/publications.pdf Version: 2024-02-01



CVF WON HAN

#	Article	IF	CITATIONS
1	Structural insights on ligand recognition at the human leukotriene B4 receptor 1. Nature Communications, 2021, 12, 2971.	12.8	13
2	Allosteric Coupling of Drug Binding and Intracellular Signaling in the A2A Adenosine Receptor. , 2021, , 184-196.		0
3	An orthogonal seryl-tRNA synthetase/tRNA pair for noncanonical amino acid mutagenesis in Escherichia coli. Bioorganic and Medicinal Chemistry, 2020, 28, 115662.	3.0	10
4	Structural basis of the activation of a metabotropic GABA receptor. Nature, 2020, 584, 298-303.	27.8	92
5	Full-length human GLP-1 receptor structure without orthosteric ligands. Nature Communications, 2020, 11, 1272.	12.8	83
6	Structural basis of ligand binding modes at the human formyl peptide receptor 2. Nature Communications, 2020, 11, 1208.	12.8	58
7	Determination of the melanocortin-4 receptor structure identifies Ca ²⁺ as a cofactor for ligand binding. Science, 2020, 368, 428-433.	12.6	89
8	Harnessing the power of an X-ray laser for serial crystallography of membrane proteins crystallized in lipidic cubic phase. IUCrJ, 2020, 7, 976-984.	2.2	15
9	Structure-based mechanism of cysteinyl leukotriene receptor inhibition by antiasthmatic drugs. Science Advances, 2019, 5, eaax2518.	10.3	71
10	A Single Reactive Noncanonical Amino Acid Is Able to Dramatically Stabilize Protein Structure. ACS Chemical Biology, 2019, 14, 1150-1153.	3.4	15
11	Structural basis of ligand recognition at the human MT1 melatonin receptor. Nature, 2019, 569, 284-288.	27.8	140
12	XFEL structures of the human MT2 melatonin receptor reveal the basis of subtype selectivity. Nature, 2019, 569, 289-292.	27.8	106
13	Molecular Mechanism for Ligand Recognition and Subtype Selectivity of α2C Adrenergic Receptor. Cell Reports, 2019, 29, 2936-2943.e4.	6.4	17
14	Elucidating the active δ-opioid receptor crystal structure with peptide and small-molecule agonists. Science Advances, 2019, 5, eaax9115.	10.3	81
15	Structural basis of ligand selectivity and disease mutations in cysteinyl leukotriene receptors. Nature Communications, 2019, 10, 5573.	12.8	47
16	Structural Basis of the Diversity of Adrenergic Receptors. Cell Reports, 2019, 29, 2929-2935.e4.	6.4	30
17	Crystal Structure of the Human Cannabinoid Receptor CB2. Cell, 2019, 176, 459-467.e13.	28.9	268
18	Crystal structure of misoprostol bound to the labor inducer prostaglandin E2 receptor. Nature Chemical Biology, 2019, 15, 11-17.	8.0	32

#	Article	IF	CITATIONS
19	Toward G protein-coupled receptor structure-based drug design using X-ray lasers. IUCrJ, 2019, 6, 1106-1119.	2.2	53
20	5-HT2C Receptor Structures Reveal the Structural Basis of GPCR Polypharmacology. Cell, 2018, 172, 719-730.e14.	28.9	185
21	Structural Connection between Activation Microswitch and Allosteric Sodium Site in GPCR Signaling. Structure, 2018, 26, 259-269.e5.	3.3	134
22	Allosteric Coupling of Drug Binding and Intracellular Signaling in the A2A Adenosine Receptor. Cell, 2018, 172, 68-80.e12.	28.9	173
23	Structure of the Nanobody-Stabilized Active State of the Kappa Opioid Receptor. Cell, 2018, 172, 55-67.e15.	28.9	299
24	Structural basis for signal recognition and transduction by platelet-activating-factor receptor. Nature Structural and Molecular Biology, 2018, 25, 488-495.	8.2	58
25	Crystal structure of the Frizzled 4 receptor in a ligand-free state. Nature, 2018, 560, 666-670.	27.8	77
26	Advances in Structure Determination of G Protein-Coupled Receptors by SFX. , 2018, , 301-329.		2
27	Generation of an Orthogonal Protein–Protein Interface with a Noncanonical Amino Acid. Journal of the American Chemical Society, 2017, 139, 5728-5731.	13.7	18
28	Structure of the full-length glucagon class B G-protein-coupled receptor. Nature, 2017, 546, 259-264.	27.8	179
29	Human GLP-1 receptor transmembrane domain structure in complex with allosteric modulators. Nature, 2017, 546, 312-315.	27.8	192
30	Crystal structure of a multi-domain human smoothened receptor in complex with a super stabilizing ligand. Nature Communications, 2017, 8, 15383.	12.8	81
31	Structural Basis for Apelin Control of the Human Apelin Receptor. Structure, 2017, 25, 858-866.e4.	3.3	96
32	Structure of CC Chemokine Receptor 5 with a Potent Chemokine Antagonist Reveals Mechanisms of Chemokine Recognition and Molecular Mimicry by HIV. Immunity, 2017, 46, 1005-1017.e5.	14.3	148
33	Structural basis for selectivity and diversity in angiotensin II receptors. Nature, 2017, 544, 327-332.	27.8	174
34	Structural insights into the extracellular recognition of the human serotonin 2B receptor by an antibody. Proceedings of the National Academy of Sciences of the United States of America, 2017, 114, 8223-8228.	7.1	54
35	Crystal structures of agonist-bound human cannabinoid receptor CB1. Nature, 2017, 547, 468-471.	27.8	379
36	Structural insights into the molecular mechanisms of myasthenia gravis and their therapeutic implications. ELife, 2017, 6, .	6.0	22

#	Article	IF	CITATIONS
37	Structure of CC chemokine receptor 2 with orthosteric and allosteric antagonists. Nature, 2016, 540, 458-461.	27.8	220
38	Native phasing of x-ray free-electron laser data for a G protein–coupled receptor. Science Advances, 2016, 2, e1600292.	10.3	97
39	X-ray laser diffraction for structure determination of the rhodopsin-arrestin complex. Scientific Data, 2016, 3, 160021.	5.3	51
40	Crystal Structure of the Human Cannabinoid Receptor CB1. Cell, 2016, 167, 750-762.e14.	28.9	468
41	Exploring the potential impact of an expanded genetic code on protein function. Proceedings of the National Academy of Sciences of the United States of America, 2015, 112, 6961-6966.	7.1	69
42	Trapping a transition state in a computationally designed protein bottle. Science, 2015, 347, 863-867.	12.6	36
43	Structural basis for bifunctional peptide recognition at human δ-opioid receptor. Nature Structural and Molecular Biology, 2015, 22, 265-268.	8.2	151
44	Crystal structure of the chemokine receptor CXCR4 in complex with a viral chemokine. Science, 2015, 347, 1117-1122.	12.6	325
45	Crystal Structure of Antagonist Bound Human Lysophosphatidic Acid Receptor 1. Cell, 2015, 161, 1633-1643.	28.9	169
46	Crystal structure of rhodopsin bound to arrestin by femtosecond X-ray laser. Nature, 2015, 523, 561-567.	27.8	683
47	Structure of the Angiotensin Receptor Revealed by Serial Femtosecond Crystallography. Cell, 2015, 161, 833-844.	28.9	315
48	Two disparate ligand-binding sites in the human P2Y1 receptor. Nature, 2015, 520, 317-321.	27.8	305
49	The Importance of Ligand-Receptor Conformational Pairs in Stabilization: Spotlight on the N/OFQ G Protein-Coupled Receptor. Structure, 2015, 23, 2291-2299.	3.3	64
50	Structural Basis for Ligand Recognition and Functional Selectivity at Angiotensin Receptor. Journal of Biological Chemistry, 2015, 290, 29127-29139.	3.4	145
51	Structure of a Class C GPCR Metabotropic Glutamate Receptor 1 Bound to an Allosteric Modulator. Science, 2014, 344, 58-64.	12.6	476
52	Lipidic cubic phase injector facilitates membrane protein serial femtosecond crystallography. Nature Communications, 2014, 5, 3309.	12.8	505
53	Structure of the human P2Y12 receptor in complex with an antithrombotic drug. Nature, 2014, 509, 115-118.	27.8	330
54	Structural basis for Smoothened receptor modulation and chemoresistance to anticancer drugs. Nature Communications, 2014, 5, 4355.	12.8	208

#	Article	IF	CITATIONS
55	Agonist-bound structure of the human P2Y12 receptor. Nature, 2014, 509, 119-122.	27.8	279
56	Structure of the human glucagon class B G-protein-coupled receptor. Nature, 2013, 499, 444-449.	27.8	352
57	The Role of a Sodium Ion Binding Site in the Allosteric Modulation of the A2A Adenosine G Protein-Coupled Receptor. Structure, 2013, 21, 2175-2185.	3.3	118
58	Serial Femtosecond Crystallography of G Protein–Coupled Receptors. Science, 2013, 342, 1521-1524.	12.6	424
59	Structure of the CCR5 Chemokine Receptor–HIV Entry Inhibitor Maraviroc Complex. Science, 2013, 341, 1387-1390.	12.6	606
60	Structural Features for Functional Selectivity at Serotonin Receptors. Science, 2013, 340, 615-619.	12.6	600
61	Structural Basis for Molecular Recognition at Serotonin Receptors. Science, 2013, 340, 610-614.	12.6	454
62	Structure of the human smoothened receptor bound to an antitumour agent. Nature, 2013, 497, 338-343.	27.8	415
63	Crystal structure of a voltage-gated K+ channel pore module in a closed state in lipid membranes Journal of Biological Chemistry, 2013, 288, 3476.	3.4	Ο
64	Crystal Structure of a Voltage-gated K+ Channel Pore Module in a Closed State in Lipid Membranes. Journal of Biological Chemistry, 2012, 287, 43063-43070.	3.4	21
65	Structural Basis for Allosteric Regulation of GPCRs by Sodium Ions. Science, 2012, 337, 232-236.	12.6	860
66	Crystal Structure of a Lipid G Protein–Coupled Receptor. Science, 2012, 335, 851-855.	12.6	600
67	Functional and structural characterization of a thermostable acetyl esterase from <i>Thermotoga maritima</i> . Proteins: Structure, Function and Bioinformatics, 2012, 80, 1545-1559.	2.6	46
68	Structure of the human \hat{I}^{e} -opioid receptor in complex with JDTic. Nature, 2012, 485, 327-332.	27.8	797
69	Structure of an Agonist-Bound Human A _{2A} Adenosine Receptor. Science, 2011, 332, 322-327.	12.6	783
70	Structure of the human histamine H1 receptor complex with doxepin. Nature, 2011, 475, 65-70.	27.8	727
71	Crystal structure of a metalâ€dependent phosphoesterase (YP_910028.1) from <i>Bifidobacterium adolescentis</i> : Computational prediction and experimental validation of phosphoesterase activity. Proteins: Structure, Function and Bioinformatics, 2011, 79, 2146-2160.	2.6	11
72	The crystal structure of a bacterial Sufuâ€like protein defines a novel group of bacterial proteins that are similar to the Nâ€terminal domain of human Sufu. Protein Science, 2010, 19, 2131-2140.	7.6	12

#	Article	IF	CITATIONS
73	Crystal structure of soluble MD-1 and its interaction with lipid IVa. Proceedings of the National Academy of Sciences of the United States of America, 2010, 107, 10990-10995.	7.1	37
74	Structure of the Human Dopamine D3 Receptor in Complex with a D2/D3 Selective Antagonist. Science, 2010, 330, 1091-1095.	12.6	1,034
75	Bacterial Pleckstrin Homology Domains: A Prokaryotic Origin for the PH Domain. Journal of Molecular Biology, 2010, 396, 31-46.	4.2	32
76	Crystal Structure of the First Eubacterial Mre11 Nuclease Reveals Novel Features that May Discriminate Substrates During DNA Repair. Journal of Molecular Biology, 2010, 397, 647-663.	4.2	41
77	Structural and Functional Characterizations of SsgB, a Conserved Activator of Developmental Cell Division in Morphologically Complex Actinomycetes. Journal of Biological Chemistry, 2009, 284, 25268-25279.	3.4	23
78	Structural Basis of Murein Peptide Specificity of a γ-D-Glutamyl-L-Diamino Acid Endopeptidase. Structure, 2009, 17, 303-313.	3.3	73
79	Crystal structure of a novel archaeal AAA+ ATPase SSO1545 from <i>Sulfolobus solfataricus</i> . Proteins: Structure, Function and Bioinformatics, 2009, 74, 1041-1049.	2.6	8
80	Crystal structure of the Fic (Filamentation induced by cAMP) family protein SO4266 (gi 24375750) from <i>Shewanella oneidensis</i> MRâ€l at 1.6 Ă resolution. Proteins: Structure, Function and Bioinformatics, 2009, 75, 264-271.	2.6	23
81	A Structural Basis for the Regulatory Inactivation of DnaA. Journal of Molecular Biology, 2009, 385, 368-380.	4.2	15
82	Crystal Structure of Histidine Phosphotransfer Protein ShpA, an Essential Regulator of Stalk Biogenesis in Caulobacter crescentus. Journal of Molecular Biology, 2009, 390, 686-698.	4.2	13
83	Metal ions and phosphate binding in the H-N-H motif: Crystal structures of the nuclease domain of ColE7/Im7 in complex with a phosphate ion and different divalent metal ions. Protein Science, 2009, 11, 2947-2957.	7.6	51
84	Crystal structure of AICAR transformylase IMP cyclohydrolase (TM1249) from <i>Thermotoga maritima</i> at 1.88 Ã resolution. Proteins: Structure, Function and Bioinformatics, 2008, 71, 1042-1049.	2.6	7
85	Crystal structure of an ADPâ€ribosylated protein with a cytidine deaminaseâ€like fold, but unknown function (TM1506), from <i>Thermotoga maritima</i> at 2.70 Ã resolution. Proteins: Structure, Function and Bioinformatics, 2008, 71, 1546-1552.	2.6	6
86	Crystal structures of MW1337R and lin2004: Representatives of a novel protein family that adopt a fourâ€helical bundle fold. Proteins: Structure, Function and Bioinformatics, 2008, 71, 1589-1596.	2.6	3
87	Crystal structure of homoserine O-succinyltransferase from Bacillus cereus at 2.4 Ã resolution. Proteins: Structure, Function and Bioinformatics, 2007, 68, 999-1005.	2.6	13
88	Crystal structure of NMA1982 from <i>Neisseria meningitidis</i> at 1.5 Ã resolution provides a structural scaffold for nonclassical, eukaryoticâ€like phosphatases. Proteins: Structure, Function and Bioinformatics, 2007, 69, 415-421.	2.6	11
89	Crystal structure of TM1030 from Thermotoga maritima at 2.3 Ã resolution reveals molecular details of its transcription repressor function. Proteins: Structure, Function and Bioinformatics, 2007, 68, 418-424.	2.6	5
90	Crystal structures of two novel dyeâ€decolorizing peroxidases reveal a βâ€barrel fold with a conserved hemeâ€binding motif. Proteins: Structure, Function and Bioinformatics, 2007, 69, 223-233.	2.6	81

#	Article	IF	CITATIONS
91	Crystal structure of MtnX phosphatase from <i>Bacillus subtilis</i> at 2.0 à resolution provides a structural basis for bipartite phosphomonoester hydrolysis of 2â€hydroxyâ€3â€ketoâ€5â€methylthiopentenylâ€1â€phosphate. Proteins: Structure, Function and Bioinformatic 2007, 69, 433-439.	2.6 :S,	6
92	Identification and structural characterization of heme binding in a novel dyeâ€decolorizing peroxidase, TyrA. Proteins: Structure, Function and Bioinformatics, 2007, 69, 234-243.	2.6	67
93	Crystal structure of phosphoribosylformylglycinamidine synthase II (smPurL) from Thermotoga maritima at 2.15 Ã resolution. Proteins: Structure, Function and Bioinformatics, 2006, 63, 1106-1111.	2.6	7
94	Crystal structure of TM1367 from Thermotoga maritima at 1.90 Ã resolution reveals an atypical member of the cyclophilin (peptidylprolyl isomerase) fold. Proteins: Structure, Function and Bioinformatics, 2006, 63, 1112-1118.	2.6	6
95	Crystal structure of acireductone dioxygenase (ARD) from Mus musculus at 2.06 Ã resolution. Proteins: Structure, Function and Bioinformatics, 2006, 64, 808-813.	2.6	28
96	Crystal structure of the ApbE protein (TM1553) from Thermotoga maritima at 1.58 Ã resolution. Proteins: Structure, Function and Bioinformatics, 2006, 64, 1083-1090.	2.6	10
97	Crystal structure of an ORFan protein (TM1622) fromThermotoga maritimaat 1.75 Ã resolution reveals a fold similar to the Ran-binding protein Mog1p. Proteins: Structure, Function and Bioinformatics, 2006, 65, 777-782.	2.6	7
98	Comparative structural analysis of a novel glutathioneS-transferase (ATU5508) fromAgrobacterium tumefaciensat 2.0 Ã resolution. Proteins: Structure, Function and Bioinformatics, 2006, 65, 527-537.	2.6	8
99	Structural and Biophysical Characterization of the EphB4·EphrinB2 Protein-Protein Interaction and Receptor Specificity. Journal of Biological Chemistry, 2006, 281, 28185-28192.	3.4	87
100	The Structure of a Eukaryotic Nicotinic Acid Phosphoribosyltransferase Reveals Structural Heterogeneity among Type II PRTases. Structure, 2005, 13, 1385-1396.	3.3	35
101	Crystal structure of an alanine-glyoxylate aminotransferase from Anabaena sp. at 1.70 Ã resolution reveals a noncovalently linked PLP cofactor. Proteins: Structure, Function and Bioinformatics, 2005, 58, 971-975.	2.6	14
102	Crystal structure of S-adenosylmethionine:tRNA ribosyltransferase-isomerase (QueA) from Thermotoga maritima at 2.0 A resolution reveals a new fold. Proteins: Structure, Function and Bioinformatics, 2005, 59, 869-874.	2.6	16
103	Crystal structure of an indigoidine synthase A (IndA)-like protein (TM1464) from Thermotoga maritima at 1.90 Ã resolution reveals a new fold. Proteins: Structure, Function and Bioinformatics, 2005, 59, 864-868.	2.6	13
104	Crystal structure of an Apo mRNA decapping enzyme (DcpS) from Mouse at 1.83 Ã resolution. Proteins: Structure, Function and Bioinformatics, 2005, 60, 797-802.	2.6	12
105	Crystal structure of a putative modulator of DNA gyrase (pmbA) from Thermotoga maritima at 1.95 Ã resolution reveals a new fold. Proteins: Structure, Function and Bioinformatics, 2005, 61, 444-448.	2.6	10
106	Crystal structure of the global regulatory protein CsrA from Pseudomonas putida at 2.05 Ã resolution reveals a new fold. Proteins: Structure, Function and Bioinformatics, 2005, 61, 449-453.	2.6	69
107	Crystal structure of Hsp33 chaperone (TM1394) from Thermotoga maritima at 2.20 Ã resolution. Proteins: Structure, Function and Bioinformatics, 2005, 61, 669-673.	2.6	13
108	Crystal structure of a conserved hypothetical protein (gi: 13879369) from Mouse at 1.90 Ã resolution reveals a new fold. Proteins: Structure, Function and Bioinformatics, 2005, 61, 1132-1136.	2.6	9

#	Article	IF	CITATIONS
109	Crystal structure of virulence factor CJ0248 from Campylobacter jejuni at 2.25 Ã resolution reveals a new fold. Proteins: Structure, Function and Bioinformatics, 2005, 62, 292-296.	2.6	6
110	Structure-based chemical modification strategy for enzyme replacement treatment of phenylketonuria. Molecular Genetics and Metabolism, 2005, 86, 134-140.	1.1	57
111	Crystal structure of an α/β serine hydrolase (YDR428C) from Saccharomyces cerevisiae at 1.85 Ã resolution. Proteins: Structure, Function and Bioinformatics, 2004, 58, 755-758.	2.6	11
112	An Unusual Sugar Conformation in the Structure of an RNA/DNA Decamer of the Polypurine Tract May Affect Recognition by RNase H. Journal of Molecular Biology, 2003, 334, 653-665.	4.2	42
113	Crystal structure of an RNA{middle dot}DNA hybrid reveals intermolecular intercalation: Dimer formation by base-pair swapping. Proceedings of the National Academy of Sciences of the United States of America, 2003, 100, 9214-9219.	7.1	17
114	Structural basis of non-specific lipid binding in maize lipid-transfer protein complexes revealed by high-resolution X-ray crystallography1 1Edited by D. Rees. Journal of Molecular Biology, 2001, 308, 263-278.	4.2	175
115	Direct-methods determination of an RNA/DNA hybrid decamer at 1.15â€Ã resolution. Acta Crystallographica Section D: Biological Crystallography, 2001, 57, 213-218.	2.5	8
116	Lactate dehydrogenase from the hyperthermophilic archaeon Methanococcus jannaschii: overexpression, crystallization and preliminary X-ray analysis. Acta Crystallographica Section D: Biological Crystallography, 2000, 56, 81-83.	2.5	2
117	Structure of a DNA analog of the primer for HIV-1 RT second strand synthesis 1 1Edited by P. E. Wright. Journal of Molecular Biology, 1997, 269, 811-826.	4.2	49
118	Defining GC-specificity in the minor groove: side-by-side binding of the di-imidazole lexitropsin to C-A-T-G-G-C-C-A-T-G. Structure, 1997, 5, 1033-1046.	3.3	109